Random walks in fractal media: a theoretical evaluation of the periodicity of the oscillations in dynamic observables

2008 J. Phys. A: Math. Theor. 41 495004

(http://iopscience.iop.org/1751-8121/41/49/495004)

IOP PUBLISHING JOURNAL OF PHYSICS A: MATHEMATICAL AND THEORETICAL

J. Phys. A: Math. Theor. **41** (2008) 495004 (12pp) doi:10.1088/1751-8113/41/49/495004

Random walks in fractal media: a theoretical evaluation of the periodicity of the oscillations in dynamic observables

Alberto L Maltz[1], **Gabriel Fabricius**[2], **Marisa A Bab**[2] **and Ezequiel V Albano**[2]

[1] Departamento de Matemática, Universidad Nacional de La Plata, Casilla de Correo 172 (1900) La Plata, Argentina
[2] Instituto de Investigaciones Fisicoquímicas Teóricas y Aplicadas (INIFTA), CCT La Plata, UNLP, CONICET. Casilla de Correo 16, Sucursal 4, (1900) La Plata, Argentina.

Received 21 July 2008, in final form 2 October 2008
Published 29 October 2008
Online at stacks.iop.org/JPhysA/41/495004

Abstract
In this work we address the time evolution of random walks on a special type of Sierpinski carpets, which we call walk similar (WS). By considering highly symmetric fractals (symmetrically self-similar graphs (SSG)), very recently Krön and Teufl (2003 *Trans. Am. Math. Soc.* **356** 393) have developed a technique based on the fact that the random walk gives rise to an equivalent process in a similar subset. The method is used in order to obtain the time scaling factor (τ) as the average passing time (APT) of the walker from a site in the subset to any different site in the subset. For SSG, the APT is independent of the starting point. In the present work we generalize this technique under the less stringent symmetry conditions of the WS carpets, such that the APT depends on the starting point. Therefore, we calculate exactly the weighted APT (τ^*). By performing Monte Carlo simulations on several WS carpets we verify that τ^* plays the role of τ by setting the logarithmic period of the oscillatory asymptotic behaviour of dynamic observables.

PACS numbers: 05.40.Fb, 05.45.Df, 02.50.−r, 02.70.Uu

(Some figures in this article are in colour only in the electronic version)

1. Introduction

The dynamic properties of physical systems on fractal media have caught increasing interest in the last few years [1–3]. Following the time evolution of physical observables on a fractal substrate allows one to explore the influence of symmetry and dimension of the substrate on the time behaviour of the observables. One of the most striking features of this interplay is the now well-established fact that observables exhibit logarithmic oscillations in their time evolution [4–6]. These oscillations have been reported in several contexts and they are related to discrete scale invariance (DSI) symmetry [7]. Recently, it has been proposed that dynamic observables describing physical processes on fractal substrates with spatial DSI symmetry, for both under and far-from equilibrium conditions, will exhibit logarithmic oscillations in their time evolution, i.e., time DSI, as a consequence of a developing correlation length [5].

Particularly important is the case of random walks on fractal substrates. The random walk is the paradigmatic and simplest case of a diffusive system and the study of its dynamic properties directly reflects the influence of the underlying fractal substrate. When the fractal structure has very strong symmetric conditions, some analytical proofs have been given. Grabner and Woess [8] have demonstrated that the probability of return to the origin for the specific case of a random walker on a Sierpinski gasket S has the following asymptotic expression,

$$p_0(t) = t^{-d_s/2}\left[H\left(\frac{\log(t)}{\log(\tau)}\right) + \mathcal{O}(t^{-1})\right], \tag{1}$$

where t is the number of steps, H is a smooth function of period 1, $d_s/2 = \log(3)/\log(5)$ and $\tau = 5$. The technique used in that work is based on the consideration of a similar subset S', in such a way that the random walk on the whole fractal gives rise to an equivalent process on S'. If the walk starts at a given site z' in S', the average time required to visit any different site in S' (i.e., the so-called average passing time APT) is independent of z' and its value is the time scaling factor τ. Subsequently, Teufl [9] has shown that, for this case, it is also possible to obtain an asymptotic expression for the root of the mean square distance to the origin $R^2(t)$, which is given by equation (1) but with an exponent $2/d_w = -\log(2)/\log(5)$. In 2003, Krön and Teufl [10] generalized the validity of equation (1) for a wider (but still very narrow) class of fractals, i.e., for symmetrically self-similar graphs (SSG), by showing that

$$d_s/2 = \log(\mu)/\log(\tau), \tag{2}$$

where μ is the mass scaling factor (directly determined from the fractal structure) and τ is the time scaling factor, which is also equal to the exactly determined APT (for detailed definitions, see section 2).

In the present work we deal with a class of Sierpinski carpets (with horizontal and vertical neighbours), which we call WS carpets, for which the high-symmetry conditions required by Krön and Teufl are not satisfied. However, given a WS carpet F, it is possible to find an adequate, similar sub-carpet F' by selecting a special site from each one of the 'copies' of the basic cell that make up F (see the precise definitions and details in the following section). As in the cited papers [9, 10], for WS carpets the random walk on F gives rise to an equivalent process on F', but now the APT depends on the starting site z'. Then we determine an exact weighted mean of all the individual APT values, denoting it as τ^*.

It is also worth mentioning that for the case of WS carpets, it is no longer possible to replicate the analytical technique already used in previous papers [9, 10], in order to prove the existence of logarithmic oscillations in the asymptotic behaviour of time-dependent observables. In order to overcome this shortcoming we performed numerical simulations of random walks on several WS fractal substrates, and verified that the asymptotic expressions obtained for $R^2(t)$ [10] and $p_0(t)$ [9] hold very well when τ^* is used in place of τ.

The paper is organized as follows: section 2 is devoted to the theoretical calculations, we give some basic definitions, develop our computation scheme for τ^*, and apply it to some examples. In section 3 we present the results of our numerical simulations, and in section 4 we discuss our results and give the conclusions of our work.

2. Theoretical calculations

2.1. Walk-similar carpets: definition and examples

In this subsection the conditions that have to satisfy the fractals used are specified. As in [6], deterministic carpets F generated by means of the following typical scheme will be considered: take a site z_0 (origin) and a positive integer M. Call F_0 the set having the origin as its only site. Then the minimal cell F_1 is built by following a specific geometrical procedure that adds M sites to F_0. Now, inductively, construct the set F_{n+1} by adding to the set $F_n M$ 'copies' of itself according to the same geometrical pattern. Finally, F is the union of the sets F_n for all n. F_1 is commonly called the *basic cell* or the first generation, which, in the present case, has to be minimal in the sense that it cannot be decomposed into smaller cells. The mass scaling factor is then defined as $\mu = M + 1$. Note that F can be decomposed into a union of infinite many copies of F_1. Let F' be the set constructed by picking the copy of the origin in each one of these replications of the basic cell. Due to the self-similarity of F, there exists a natural one-to-one correspondence $z \leftrightarrow z'$ between the sites $z \in F$ and $z' \in F'$.

Consider the symmetric random walk on F departing from z_0: when the walker is at some z of F, the probability to visit each neighbour site is $1/\deg_F(z)$ (where $\deg_F(z)$ = number of neighbours of z in F). Then it is defined that two sites of F' are *neighbours in* F' whenever they can be joined by a path *in* F not visiting other points of F'.

For each z' in F', the *environment of* z' *in* F is defined as the set formed by z' and the sites not belonging to F' that can be joined with z' (in F) by a path not passing by any point of F'.

Then, a connected finite ramification fractal F is defined as WS (walk-similar) if the one-to-one correspondence $z \leftrightarrow z'$ between F and F' satisfies the following properties:
(a) z_1 and z_2 are neighbours in F if and only if z'_1 and z'_2 are neighbours in F'.
(b) If z_1 and z_2 are F sites, the following probabilities are equal:
p = probability that, starting at z_1, z_2 is visited in the first step.
p' = probability that, starting at z'_1, z'_2 is the first F' site different than z'_1 1 cm visited by the walker.

The idea behind those definitions is that a walk on F has also to originate a walk on F': the walker departs from $z'_0 = z_0$, the second step of the F' walk is the next distinct F' site visited by the walker, etc. So, the WS conditions imply the presence of two equivalent stochastic processes.

The symmetry of WS carpets implies the existence of a length scaling factor b. Three examples that fulfil the conditions to be WS are given in figure 1. Here, we introduce the notation $L_{b=2}$ for the fractal whose first generation has the shape of an L with $b = 2$ (figure 1(a)), and $T_{b=3}$ for the fractal whose first generation has the shape of a T with $b = 3$ (figure 1(b)). These carpets are loopless and they will be useful in order to illustrate our procedures. Figure 1(c) shows a basic cell having a more complicate structure, which leads to a nonloopless WS carpet that we denote $LM_{b=5}$.

2.2. Local analysis

Let us first consider a fixed site w_1 in F'. Suppose that the F' sites $w_2, w_2, \ldots, w_r$ are the neighbours of w_1 *in* F', and $w_{r+1}, \ldots, w_s$ (together with w_1) form the environment of w_1 in F. Then let us assume that the symmetric random walk starts at w_1 and finishes the first arrival at some w_j, with $2 \leqslant j \leqslant r$ (as is known, this event occurs with probability 1). Define the

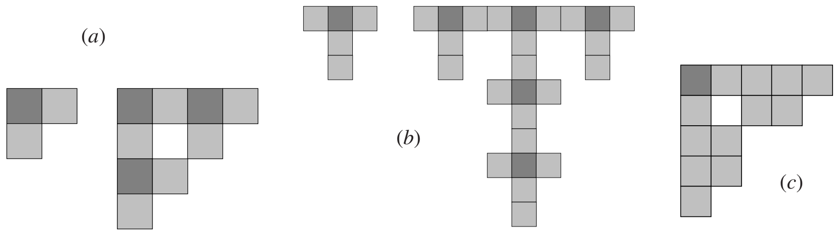

Figure 1. Examples of WS fractals: (a) fractal $F \equiv L_{b=2}$, (b) fractal $F \equiv T_{b=3}$ and (c) fractal $LM_{b=5}$. The notation for the fractals is explained in the text. In cases (a) and (b) sites belonging to the F_1 and F_2 sets are shown, while in case (c) only F_1 is shown for the sake of space. Dark grey squares indicate sites also belonging to the corresponding F' set.

ATP of w_1 ($\tau(w_1)$) as the expected number of steps of this walk. Now, in order to calculate $\tau(w_1)$ let us consider the $s \times s$ transition matrix P of this local walk given by

$P(i, j) = 0$, if w_i, w_j are not neighbours in F,
$P(i, j) = 0$, for every i, if $2 \leqslant j \leqslant r$, and
$P(i, j) = 1/\deg_F(w_j)$, if $j = 1$ or $r + 1 \leqslant j \leqslant s$ and w_i, w_j are neighbours in F.

For every integer $k \geqslant 1$, $P^k(i, j)$ is the probability that the walker will arrive at the site w_i in the step k, starting at w_j. Then, if I is the $s \times s$ identity matrix, it is well known that

$$(I - P)^{-1} = \sum_{k=0}^{\infty} P^k,$$

and this implies

$$\sum_{k=1}^{\infty} kP^k = \sum_{l=1}^{\infty}\sum_{k=l}^{\infty} P^k = \sum_{l=1}^{\infty} P^l(I - P)^{-1} = P(I - P)^{-2}.$$

Then, if $Q = P(I - P)^{-2}$, we have

$$\tau(w_1) = \sum_{i=2}^{r}\sum_{k=1}^{\infty} kP^k(i, 1) = \sum_{i=2}^{r} Q(i, 1).$$

2.3. Computation of τ^*

Let us recall that there exists only a finite number of possible geometric arrangements between each site of F and its neighbours. Then according to this criterion F can be partitioned into a finite number of subsets $A_1, \ldots, A_m$. The corresponding subsets $A'_1, \ldots, A'_m$ of F' satisfy that, for each fixed j, the sites in A'_j have an equivalent environment structure. This condition implies that the sites in A_j and in A'_j have the same number D_j of neighbours in F and in F', respectively. The converse is not true: two or more sites with the same number of neighbours can have different geometric situations (see the last solved example).

The first key fact that allows us to calculate τ^* is that all sites z' in A'_j have the same matrices P, Q for their local computations. Hence, they have also the same value $\tau(z')$, which is denoted τ_j.

The second key fact is that (due to the WS conditions) the expected frequency f_j of visits to A_j in the first process is the same as the one to A'_j in the second process.

The preceding observations lead to

$$\tau^* = \sum_{j=1}^{m} f_j\tau_j. \tag{3}$$

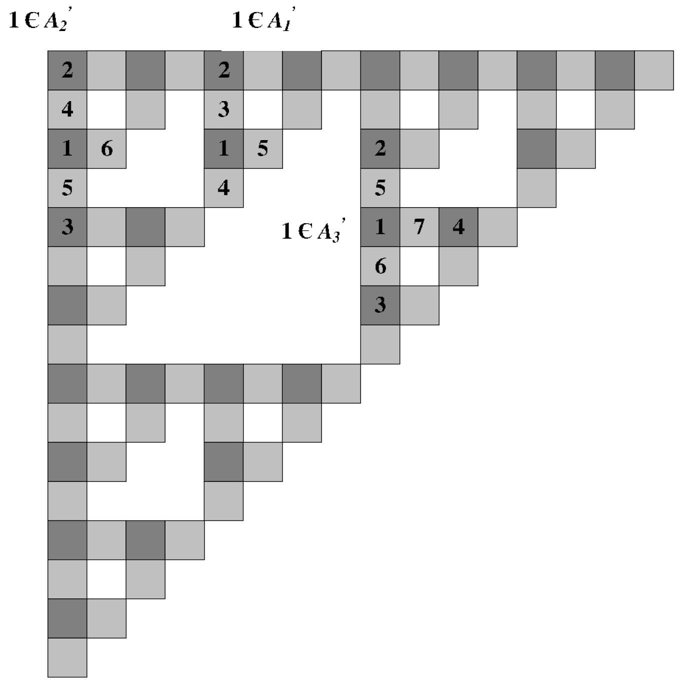

Figure 2. Sites belonging to the set F_4 for fractal $F \equiv L_{b=2}$ (first and second generations are shown in figure 1(a). Dark grey squares indicate sites belonging also to F'. The numbers have the following meaning: '1' is an F' site in A'_j; $2, 3, \ldots, r$ are its F'-neighbours and $r+1, r+2, \ldots, s$ are the sites (together with '1') belonging to the '1' environment in F. For A'_1, $r = 2$, $s = 5$; for A'_2, $r = 3$, $s = 6$; and for A'_3, $r = 4$, $s = 7$

In order to perform the calculations we propose the following scheme. For each n and j, let $c(n, j)$ be the number of F_n sites in A_j. Since the expected frequency of visits to A_j is proportional to D_j, for each j one has

$$f_j = D_j . \lim_{n\to\infty} c(n, j)/T_n, \qquad \text{where} \qquad T_n = \sum_{i=1}^{m} c(n, i) D_i. \tag{4}$$

2.4. Solved examples

In this subsection we show a sketch of the computation of τ^* for three WS carpets. In the following, matrices are not displayed for the sake of space. Let us begin with the fractal of figure 1(a). Let A_1 be sites with one neighbour, A_2 be sites with a vertical neighbour and a horizontal neighbour (the origin can be neglected because it has a special local situation), and A_3 be sites with three neighbours. Then $D_j = j$ for $j = 1, 2, 3$.

Using simple recurrence relationships we obtain $c(n, j) \sim 3^{n-1}$ for $j = 1, 2, 3$, $T_n \sim 2 \times 3^n$ (note that for an arbitrary pair of sequences u_n and v_n, we denote $u_n \sim v_n$ when the $\lim_{n\to\infty} u_n/v_n = 1$ holds), $f_1 = 1/6$, $f_2 = 1/3$ and $f_3 = 1/2$.

For each j, figure 2 shows the local structure from which τ_j is computed. The following notations are used: 1 is an F' site in A'_j; $2, 3, \ldots, r$ are its F' neighbours and $r+1, r+2, \ldots,$ s are the sites (together with '1') of the '1' environment in F.

A detailed calculation gives $\tau_1 = 12, \tau_2 = 6, \tau_3 = 4$. Finally, one has that $\tau^* = \tau_1 f_1 + \tau_2 f_2 + \tau_3 f_3 = 6$.

Let us now consider the fractal of figure 1(b) and the sets A_1 (sites with a vertical neighbour), A_2 (sites with an horizontal neighbour), A_3 (sites with two vertical neighbours), A_4 (sites with two horizontal neighbours), A_5 (sites with three neighbours) and A_6 (sites with four neighbours). The obtained results are

$$c(n,1) \sim \tfrac{1}{2} \times 5^{n-1}, \quad c(n,2) \sim 5^{n-1}, \quad c(n,3) \sim \tfrac{3}{2} \times 5^{n-1}, \quad c(n,4) \sim 5^{n-1},$$
$$c(n,5) \sim \tfrac{1}{2} \times 5^{n-1}, \quad c(n,6) \sim \tfrac{1}{2} \times 5^{n-1}, \quad T_n \sim 10 \times 5^{n-1},$$
$$f_1 = 1/20, \quad f_2 = 2/20, \quad f_3 = 6/20, \quad f_4 = 4/20, \quad f_5 = 3/20, \quad f_6 = 4/20,$$
$$\tau_1 = 33, \quad \tau_2 = 27, \quad \tau_3 = 15, \quad \tau_4 = 15, \quad \tau_5 = \tau_6 = 9 \quad \text{and finally} \quad \tau^* = 15.$$

Consider now the carpet $LM_{b=5}$, whose generating cell is shown in figure 1(c). By taking the partition composed by A_1 (sites with one neighbour), A_2 (sites with two horizontal neighbours), A_3 (sites with a vertical up neighbour and a horizontal right neighbour, or sites with a vertical down neighbour and a horizontal left neighbour), A_4 (sites with a vertical up neighbour and a horizontal left neighbour), A_5 (sites with three neighbours) and A_6 (sites with four neighbours), the calculations lead to

$$c(n,1) \sim \tfrac{5}{6} \times 13^{n-1}, \quad c(n,2) \sim \tfrac{19}{6} \times 13^{n-1}, \quad c(n,3) \sim 2 \times 13^{n-1},$$
$$c(n,4) \sim 2 \times 13^{n-1}, \quad c(n,5) \sim \tfrac{29}{6} \times 13^{n-1}, \quad c(n,6) \sim \tfrac{1}{6} \times 13^{n-1},$$
$$f_1 = 5/182, \quad f_2 = 38/182, \quad f_3 = 24/182, \quad f_4 = 24/182, \quad f_5 = 87/182,$$
$$f_6 = 4/182, \quad \tau_1 = 171, \quad \tau_2 = \tau_3 = 71.25, \quad \tau_4 = 104.5, \quad \tau_5 = \tau_6 = 38$$
and finally $\tau^* = 61.75$.

3. Numerical simulations

In this section we present the results of numerical simulations of random walkers on fractal media with the aim of comparing them to the theoretical predictions of the previous section. We use standard Monte Carlo techniques to simulate the displacement of random walkers on WS Sierpinski carpets and directly compute the average squared displacement $R^2(t)$ and the probability of returning to the origin $p_0(t)$ from the obtained trajectories. In order to obtain reliable statistics the observables are averaged over a number n_s of different trajectories. We use large enough lattices in order to guarantee that the walkers never reach the edges, so that our results are free of finite-size effects.

We fit the asymptotic behaviour of $p_0(t)$ to the expression

$$p_0(t) = t^{-d_s/2} \sum_{n=0}^{N_\omega} \alpha_n \cos\left(2\pi n \frac{\log(t)}{\log(\tau)} + \varphi_n\right), \tag{5}$$

where $d_s/2 = \log(\mu)/\log(\tau))$, φ_n are phase shifts, α_n are constants and N_ω is the number of harmonics considered. As $\mu = M + 1$ is a fixed parameter determined by the fractal structure, the fit depends basically on τ, which governs the exponent of the power law and also the period of the oscillations. It is worth mentioning that these oscillations are the signature of the time DSI and τ is the corresponding fundamental scaling ratio between timescales.

For $R^2(t)$ we basically use the same functional asymptotic expression, namely

$$R^2(t) = t^{2/d_w} \sum_{n=0}^{N_\omega} \beta_n \cos\left(2\pi n \frac{\log(t)}{\log(\tau)} + \phi_n\right), \tag{6}$$

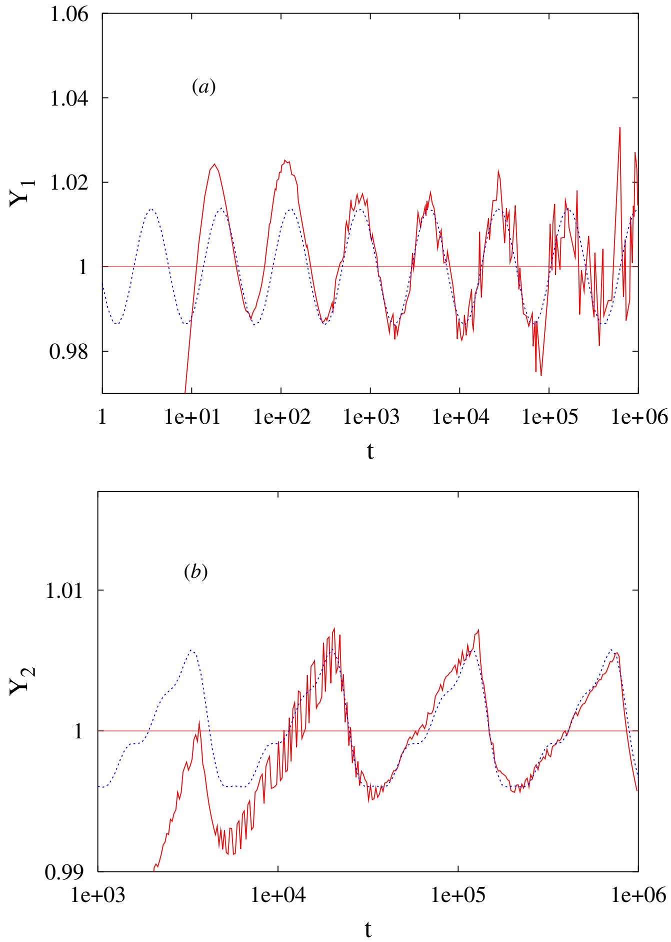

Figure 3. Temporal behaviour of dynamic observables measured for the fractal $L_{b=2}$ (generation F_{13}). (a) $Y_1 \equiv p_0/[\alpha_0 t^{-\log(\mu)/\log(\tau)}]$ for p_0 obtained from Monte Carlo simulations (continuous line) and fitted with equation (5) (dotted line) with $N_\omega = 1$, $\mu = 3$ (fixed parameter), and $\tau = 6.0$ (fitted parameter). The relative amplitude of the oscillation is given by $\alpha_1/\alpha_0 = 0.014$. (b) $Y_2 \equiv R^2/[\beta_0 t^{\log(b^2)/\log(\tau)}]$ for R^2 obtained from simulations (continuous line) and fitted with equation (6) (dotted line) with $N_\omega = 4$, $b = 2$ (fixed parameter) and $\tau = 6.0$ (fitted parameter). The amplitude of the oscillation is 0.005 ($\beta_1/\beta_0 = 0.004$, while the contributions of β_2, β_3 and β_4 are smaller than 0.001).

where the exponent is related to τ through other fixed parameters according to

$$\gamma = \frac{2}{d_w} = \frac{2}{d_f}\log(\mu)/\log(\tau), \tag{7}$$

where d_f is the fractal dimension and d_w is the random walk exponent. We propose this fitting expression as a generalization of the one demonstrated analytically for the Sierpinski gasket in [9], where $d_f = \log(\mu)/\log(2)$. Note that for Sierpinski carpets $d_f = \log(\mu)/\log(b)$, where b is the length of the side of the unit cell (measured in units of the lattice spacing), so one has

$$d_w = \log(\tau)/\log(b). \tag{8}$$

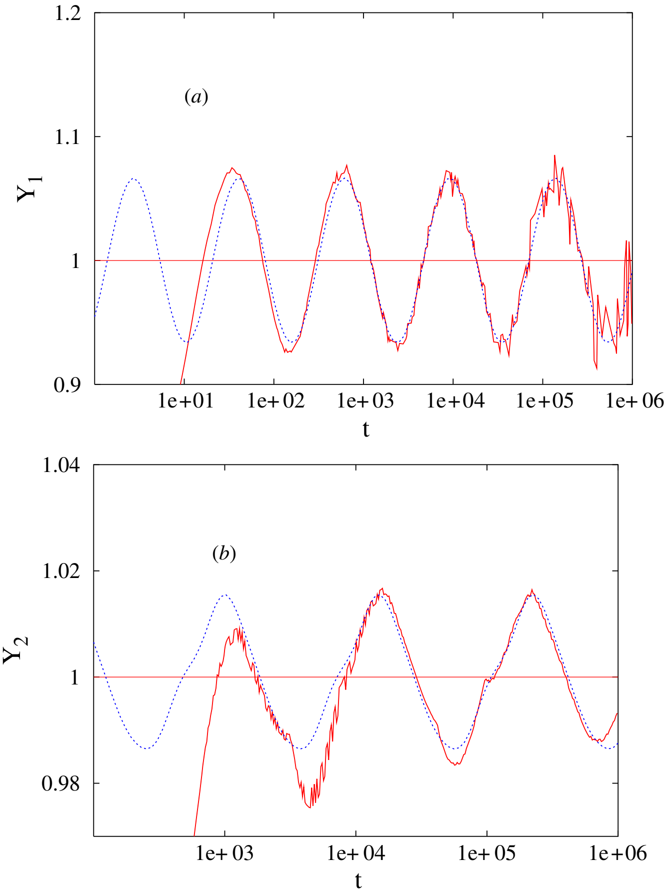

Figure 4. Same as figure 3 for the fractal $T_{b=3}$ (generation F_8). In this case, the parameters are: (a) $\mu = 5$ (fixed), $\tau = 15.0$ (fitted) and $\alpha_1/\alpha_0 = 0.07$; (b) $b = 3$ (fixed) and $\tau = 15.0$ (fitted). The amplitude of the oscillation is 0.018 ($\beta_1/\beta_0 = 0.014$, while the contributions of β_2, β_3 and β_4 are smaller than 0.001).

We first show the numerical results for the fractal $L_{b=2}$ whose basic cell F_1 is shown in figure 1(a). We performed the simulations by using the generation F_{13}, which requires a lattice of side 8192. The observables are averaged over $n_s = 10^7$ different trajectories always initialized in the origin. It should be mentioned that by starting random walks from different sites, both the amplitudes and the phases will change, but the exponents and τ remain unchanged. Figure 3 shows the time dependence of both $p_0(t)$ and $R^2(t)$. We fit the numerical data by taking $N_w = 1$ for $p_0(t)$ and $N_w = 4$ for $R^2(t)$. The data are plotted in a way that enhances the visualization of the oscillating behaviour of the observables. We chose the range of the fit from $t = 10^4$ to $t = 10^6$ since equations (5) and (6) are expected to be valid in the asymptotic regime. However, from figure 3, it is clear that the asymptotic regime is reached earlier for observable $p_0(t)$ than for $R^2(t)$. The fits give $\tau = 6.0(p_0(t))$ and $\tau = 6.0(R^2(t))$, which are in excellent agreement with the theoretically predictions of section 2.4, namely $\tau = 6$.

Figure 4 shows the results obtained for another fractal analysed in section 2.4, namely the $T_{b=3}$ fractal whose basic cell is shown in figure 1(b). The calculations are performed

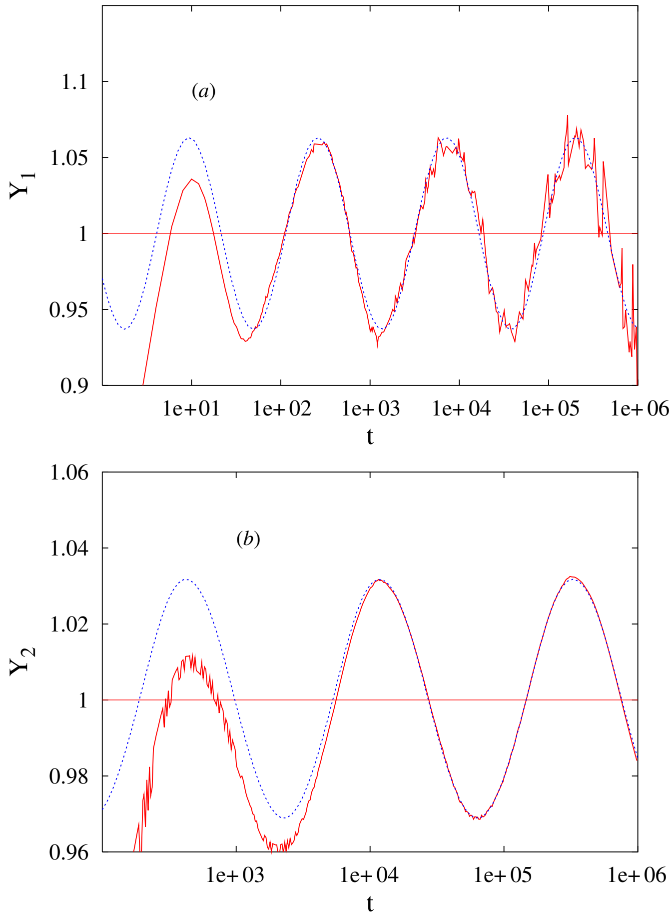

Figure 5. Same as figure 3 for the fractal $L_{b=4}$ (generation F_6). In this case, the parameters are: (a) $\mu = 7$ (fixed), $\tau = 27.8$ (fitted), and $\alpha_1/\alpha_0 = 0.06$; (b) $b = 4$ (fixed) and $\tau = 27.9$ (fitted). The amplitude of the oscillation is 0.031 ($\beta_1/\beta_0 = 0.032$, while the contributions of β_2, β_3 and β_4 are smaller than 0.0005).

for the generation F_8 (lattice of side 6561). In this case (and all the other ones presented in this section, unless explicitly indicated) we perform the fit in the range $10^3 \leqslant t \leqslant 10^6$ for observable $p_0(t)$ and $10^4 \leqslant t \leqslant 10^6$ for observable $R^2(t)$. Proceeding in this way, the range of the fit for $p_0(t)$ includes at least two complete oscillations for this observable whose statistics is poorer than that of $R^2(t)$. Furthermore, figures 5 and 6 show simulation results for the $L_{b=4}$ and $LM_{b=5}$ fractals, respectively.

Table 1 summarizes the results obtained for τ in the simulations, which are also compared with the values of τ^* obtained theoretically, showing an excellent agreement. In fact, we expect that the small differences between the values of τ and τ^* would be within the numerical error bars involved in the determination of τ. The error in τ arises because equations (5) and (6) hold in the asymptotic regime, which on the one hand is difficult to identify in the numerical simulations, and on the other hand it may be different for different fractals and different observables. For example, for fractal $LM_{b=5}$ we have enough statistics to obtain a very good fit to $R^2(t)$ in the range $10^5 \leqslant t \leqslant 5.10^6$, as can be appreciated in figure 6(b),

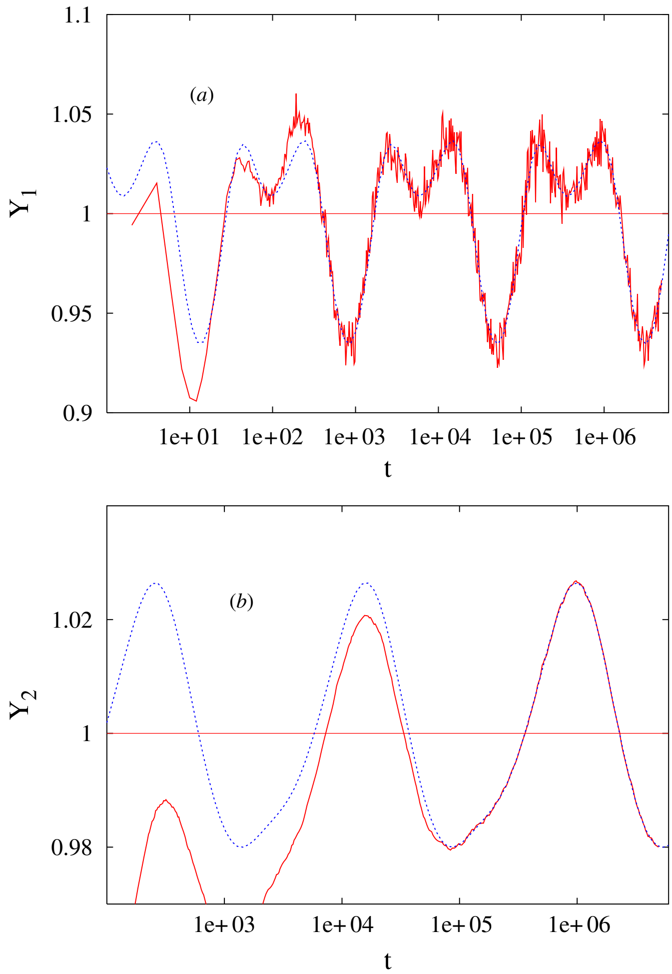

Figure 6. Same as figure 3 for the nonloopless WS fractal $LM_{b=5}$ (generation F_5). In this case, the parameters are (a) $N_\omega = 4$, $\mu = 13$ (fixed), and $\tau = 61.6$ (fitted). The amplitude of the oscillation is 0.04 ($\alpha_1/\alpha_0 = 0.037, \alpha_2/\alpha_0 = 0.029$, while the contributions of α_3 and α_4 are smaller than 0.001). (b) $N_\omega = 4$, $b = 5$ (fixed), and $\tau = 61.8$ (fitted). The amplitude of the oscillation is 0.027 ($\beta_1/\beta_0 = 0.022$, $\beta_1/\beta_0 = 0.004$, while the contributions of β_3 and β_4 are smaller than 0.001).

leading to the predicted value of $\tau \equiv \tau^*$. After a careful study of the dependence of the fitted value of τ on the range of the fit and the statistics, we can state the error bars are always smaller than 1%.

4. Discussion and conclusions

Focusing our attention on Walk Similar (WS) fractals, defined in this paper, we calculated exactly the weighted average passing time (τ^*) required by a walker to pass from a site in an adequate subset to any different site in the same subset. Subsequently, by means of extensive computer simulations, we show that τ^* can be identified with the logarithmic period of the oscillations that modulate the asymptotic behaviour of dynamic observables, such as the

Table 1. Values of weighted APT (τ^*) obtained by applying the theoretical scheme developed in section 2, and the time scaling factor (τ) obtained by fitting numerical results of Monte Carlo simulations with the aid of equations (5) and (6) for observables p_0 and R^2, respectively (for more details, see section 3).

Fractal	τ^*	τ p_0	R^2
$L_{b=2}$	6	6.0 (1)	6.0 (1)
$T_{b=3}$	15	15.0 (1)	15.0 (1)
$L_{b=4}$	28	27.8 (2)	27.9 (2)
$LM_{b=5}$	61.75	61.6 (2)	61.8 (3)

Table 2. Theoretical prediction of dynamic exponents from a fractal structure. Walker dimension, d_w, and spectral dimension, d_s, predicted from structural parameters: μ (mass scaling factor), d_f (fractal dimension) and τ^* (weighted APT). Results obtained by assuming that relationships (7) and (2) hold for WS fractals and that the time scaling factor τ is given by τ^*.

Fractal	μ	$d_f = \log(\mu)/\log(b)$	τ^*	$d_w = \log(\tau^*)/\log(b)$	$d_s/2 = \log(\mu)/\log(\tau^*)$
$L_{b=2}$	3	1.585	6	2.585	0.613
$T_{b=3}$	5	1.465	15	2.465	0.594
$L_{b=4}$	7	1.404	28	2.404	0.584
$LM_{b=5}$	13	1.594	61.75	2.562	0.622

probability of return to the origin (p_0, see equation (1)) and the average squared displacement from the origin of the walk (R^2). In this way we test that $\tau^* \equiv \tau$, i.e, the time scaling factor. In addition, our simulations validate the functional form of the asymptotic behaviour theoretically developed by Grabner and Woess [8] and Krön and Teufl [10] for fractals of higher symmetry than the WS carpets defined in this paper. Of course, τ also enters in the expressions of the exponent $d_s/2$ (see equation (2)) and d_w (see equation (7)), governing the power-law dependence of R^2 and p_0, respectively.

Let us now discuss the relationship between dynamic and static exponents. In [12] (see equation (15) and subsequent lines) it is proved that

$$\tau = b^{d_f+\zeta} \tag{9}$$

holds for finite ramified Sierpinski carpets, which implies the validity of the Einstein relationship

$$d_w = d_f + \zeta, \tag{10}$$

with ζ being the resistance scaling exponent (whose definition is detailed below).
The inspection of table 2 suggests that in the case of WS loopless carpets

$$\tau = b\mu. \tag{11}$$

This relationship can be proved by following the technique used in [12], where given a carpet G, an adequate nested sequence of similar sub-carpets $G = G^{(1)} \supset G^{(2)} \ldots$ is taken (in the case of a WS carpet F, this corresponds to $F \supset F' \ldots$). Then, if x and y are different $G^{(j)}$ sites, we considered the effective resistance R^j_{xy}, which (regarding the G sites as the nodes of an electrical network) coincides with the potential difference when a unitary current source is inserted between x and y through G. According to equation (12) in [12], for all x, y one has

$$\lim_{j\to\infty} \frac{R^{j+1}_{xy}}{R^j_{xy}} = b^{\zeta}. \tag{12}$$

Now, given two different sites of a loopless carpet, there is only one non-overlapping path between them, so their potential difference is simply their Pythagorean distance. For loopless WS carpets, the construction process ensures that, for all j, $R_{xy}^{j+1}/R_{xy}^{j} = b$. Then, according to equation (12), one has $\zeta = 1$. This fact, along with $d_f = \log(\mu)/\log(b)$ and equation (9), gives equation (11).

In the nonloopless example we obtained $\tau^* = 61.75 \neq \mu.b = 13 \times 5 = 65$, and then equation (11) does not hold. Consequently, in this case, $\zeta \neq 1$. In fact, here one has $d_w = 2.5618$, $d_f = 1.5937$, so that $\zeta = 0.9681$.

Let us now stress the relevance of the exact evaluation of τ performed in this paper because for WS fractals in general and according to equation (8), d_w assumes a meaningful physical interpretation as the exponent linking time and space fundamental scaling ratios. Also, for WS loopless fractals, one can write d_s as a function of d_w, so that both exponents of the random walk are functions of the time scaling ratio.

Finally, it should be mentioned that the observation of oscillation in time-dependent observables of the random walk is a consequence of the interplay between the space discrete scale invariance (DSI) [7] of the underlying substrate and the dynamics/kinetics of the physical process that takes place on the substrate, which leads to the occurrence of time DSI. Of course, this phenomenon is quite general and has been reported upon the relaxation of the magnetization on the Ising magnet [4], epidemic spreading in the contact process [15] and the voter model for opinion formation of a society of interacting individuals [16]. So, we expect that our study based on both exact calculations and numerical simulations will contribute to the understanding of these observations, which are yet mainly based on computer calculations only.

Acknowledgments

This work is supported financially by CONICET, UNLP and ANPCyT (Argentina). GF acknowledges the International Centre of Theoretical Physics (ICTP) for working facilities.

References

[1] Scott A (ed) 2005 *Encyclopedia of Nonlinear Science* (New York: Routledge)
[2] Avraham D B and Havlin S 2000 *Diffusion and Reactions in Fractals and Disordered Media* (Cambridge: Cambridge University Press)
[3] Weiss G H 1995 A primer of random walkology *Fractals in Science* ed A Bunde and S Havlin (Berlin: Springer) p 119
[4] Bab M A, Fabricius G and Albano E V 2006 *Phys. Rev.* E **74** 041123
[5] Bab M A, Fabricius G and Albano E V 2008 *Europhys. Lett.* **81** 10003
[6] Bab M A, Fabricius G and Albano E V 2008 *J. Chem. Phys.* **128** 044911
[7] Sornette D 1998 *Phys. Rep.* **297** 239
[8] Grabner P J and Woess W 1997 *Stoch. Proc. Appl.* **69** 127
[9] Teufl E 2003 *Comb. Probab. Comput.* **12** 203
[10] Krön B and Teufl E 2004 *Trans. Am. Math. Soc.* **356** 393
[11] Havlin S and Avraham D B 1987 *Adv. Phys.* **36** 695
[12] Franz A, Schulzky C and Hoffmann K H 2001 *Nonlinearity* **14** 1411
[13] Alexander S and Orbach R 1982 *J. Phys. Lett. (Paris)* **43** L625
[14] Rammal R and Toulouse G 1983 *J. Phys. Lett. (Paris)* **44** L13
[15] Bab M and Albano E V 2008 *J. Phys. A: Math. Theor.* **41** 045001
[16] Bab M and Albano E V 2008 *Euro. Phys. J.* B **63** 521